Journal of Hazardous Materials 181 (2010) 755–762

Contents lists available at ScienceDirect

Journal of Hazardous Materials

journal homepage: www.elsevier.com/locate/jhazmat

Adsorption of methyl orange from aqueous solution onto calcined Lapindo volcanic mud

Aishah A. Jalil[a,*], Sugeng Triwahyono[b], S. Hazirah Adam[a], N. Diana Rahim[a], M. Arif A. Aziz[a], N. Hanis H. Hairom[c], N. Aini M. Razali[a], Mahani A.Z. Abidin[a], M. Khairul A. Mohamadiah[a]

[a] Department of Chemical Engineering, Faculty of Chemical and Natural Resources Engineering, Universiti Teknologi Malaysia, 81310 UTM Skudai, Johor, Malaysia
[b] Ibnu Sina Institute for Fundamental Science Studies, Universiti Teknologi Malaysia, 81310 UTM Skudai, Johor, Malaysia
[c] Department of Water and Environmental Engineering, Faculty of Civil and Environmental Engineering, Universiti Tun Hussein Onn Malaysia, 86400 Parit Raja, Batu Pahat, Johor, Malaysia

ARTICLE INFO

Article history:
Received 25 January 2010
Received in revised form 3 May 2010
Accepted 17 May 2010
Available online 24 May 2010

Keywords:
Adsorption
Methyl orange
Lapindo volcanic mud

ABSTRACT

In this study, calcined Lapindo volcanic mud (LVM) was used as an adsorbent to remove an anionic dye, methyl orange (MO), from an aqueous solution by the batch adsorption technique. Various conditions were evaluated, including initial dye concentration, adsorbent dosage, contact time, solution pH, and temperature. The adsorption kinetics and equilibrium isotherms of the LVM were studied using pseudo-first-order and -second-order kinetic equations, as well as the Freundlich and Langmuir models. The experimental data obtained with LVM fits best to the Langmuir isotherm model and exhibited a maximum adsorption capacity (q_{max}) of 333.3 mg g^{-1}; the data followed the second-order equation. The intraparticle diffusion studies revealed that the adsorption rates were not controlled only by the diffusion step. The thermodynamic parameters, such as the changes in enthalpy, entropy, and Gibbs free energy, showed that the adsorption is endothermic, random and spontaneous at high temperature. The results indicate that LVM adsorbs MO efficiently and could be utilized as a low-cost alternative adsorbent for the removal of anionic dyes in wastewater treatment.

1. Introduction

Many textile and printing industries that use dyes and pigments release a large amount of highly colored effluent in their wastewater. Improper treatment and discharge of this wastewater into receiving streams can cause damage to the environment because the dyes prevent sunlight and oxygen penetration, and therefore, they can significantly affect photosynthetic activity in aquatic systems [1]. In addition, some dyes degrade into compounds that have toxic, mutagenic or carcinogenic influences on living organisms. Azo dyes can be particularly toxic upon degradation, and this class of dyes is widely used in many industries today [2].

Various techniques have been used to remove dyes from colored wastewater, including biological treatment, adsorption, chemical oxidation, coagulation, membrane filtration and photochemical degradation. Among them, adsorption has become the most popular technique because of its effectiveness, operational simplicity, low cost and low energy requirements. In the past few years, many waste materials or by-products have been investigated as adsorbents for removing dyes from water; some examples include fly ash [3], wheat straw [4], banana pith [5], sugar cane dust [6], and sludge [7]. The use of clay materials such as montmorillonite [8], zeolite [9], bentonite [10] and kaolinite [11] as adsorbents also has received much attention because the unique structural and surface properties of these materials offer high chemical stabilities and specific surface areas that lead to high adsorption capacities [12].

Lapindo mud (known as LUSI) is the type of volcanic mud that covers an area of >6.5 km^2 and has dislocated >30,000 people since the volcano's first eruption on May 29, 2006 in the subdistrict of Porong, Sidoarjo in East Java, Indonesia [13]. As of October 30, 2008, the mud is flowing at a rate of 100,000 m^3 (3,520,000 cubic feet) per day, and this rate is expected to continue for the next 30 years [14]. At the moment, the mud flow is contained by levees, but further breakouts are possible. Therefore, finding uses for the mud, especially on an industrial scale, would be beneficial from environmental and economical points of view.

The aim of the present work is to investigate the possibility of using Lapindo volcanic mud (LVM) for the adsorptive removal of methyl orange (MO) from aqueous solution. MO serves as a model compound for common water-soluble azo dyes, which are widely used in chemical, textile and paper industries. These dyes are particularly harmful to the environment. The adsorption efficiency of MO was studied by optimizing experimental variables such as

* Corresponding author. Tel.: +60 7 5535581; fax: +60 7 5581463.
E-mail addresses: aishah@fkkksa.utm.my, aishah_aj@yahoo.com (A.A. Jalil).

0304-3894/$ – see front matter © 2010 Elsevier B.V. All rights reserved.
doi:10.1016/j.jhazmat.2010.05.078

initial MO concentration, LVM dosage, solution pH and temperature. The properties of LVM were characterized by XRD, surface area analysis and FESEM. The reaction kinetics and thermodynamics for the adsorption were also investigated. As the best to our knowledge, this is a novel study on LVM for adsorption of dyes.

2. Experimental

2.1. Materials

LVM is dry, grey-colored clay and was purchased from Sidoarjo, Indonesia. It was calcined at 550 °C prior to use to remove water and hydrocarbons. LVM was sieved by using a sieve set and then was collected in the range of 104 and 150 μm. Analytical grade methyl orange ($C_{14}H_{14}N_3NaO_3S$; molecular weight 327.33) was obtained from Merck and was used as received. The dye solution was prepared at the desired concentration using Milli-Q water.

2.2. Characterization of LVM

The composition of LVM was determined on a Bruker AXS (S4 Pioneer) X-ray fluorescence spectrometer, and the crystalline structure was obtained on a Bruker AXS D8 Automatic Powder Diffractometer using Cu Kα radiation with λ = 1.5418 Å at 40 kV and 40 mA, over the range of 2θ = 0–40°. The specific surface area of the LVM was measured using the Brunauer–Emmet–Teller (BET) method. The results were obtained by means of the N_2 adsorption at 77 ± 0.5 K using a Quantachrome Autosorb-1 analyzer. Prior to analysis, all samples were degassed under vacuum at 110 °C for 12 h. The morphological features and surface characteristics of the samples were obtained from field emission scanning electron microscopy (FESEM) using a JEOUL JSM-6701F scanning electron microscope at an accelerating voltage of 15 kV. The samples were coated with platinum by electro-deposition under vacuum prior to analyses.

2.3. Batch adsorption experiments

Adsorption measurements on LVM were carried out in batches. A desired amount of the adsorbent was added to 50 mL of the MO solution (various concentrations). The desired pH was achieved by adjustment with 0.1 M HCl or 0.1 M NaOH. The mixture was stirred magnetically at room temperature and 300 rpm, and samples were withdrawn from the experimental flask at pre-determined time intervals until the adsorption equilibrium was reached. Next, the dye solution was separated from the adsorbent by centrifugation (Mikro 120, Hettich, UK) at 13,200 rpm for 20 min. The supernatants were filtered using a Millex-HN filter (Millipore 0.45 mm) to ensure that the solutions were free of adsorbent particles prior to measuring the residual dye concentration. All experiments were carried out in triplicate.

2.4. Dye concentration and removal capacity

The concentration of MO was determined spectrophotometrically using a UV–visible spectrophotometer (model Genesys 10 UV/Vis Scanning, Thermo Electron, UK) by taking measurements at the absorbance maximum (478 nm). A calibration curve was plotted between the absorbance and the concentration of the MO solution to obtain the absorbance–concentration profile. The amount of MO uptake per unit of adsorbent (q) was calculated using the following equations:

$$q = (C_i - C_e) \times \frac{V}{m} \quad (1)$$

Table 1
Physical and chemical properties of Lapindo volcanic mud.

Constituent	wt.%
SiO_2	53.40
Al_2O_3	23.80
Na_2O	5.59
Fe_2O_3	5.47
Cl	2.89
MgO	2.62
CaO	2.40
K_2O	1.63
SO_3	1.24
TiO_2	0.63
Specific surface area	45.59 $m^2\,g^{-1}$

where C_i is the initial MO concentration (mg L^{-1}), C_e is the MO concentration at the adsorption equilibrium (mg L^{-1}), V is the volume of MO solution (L), and m is the weight of the LVM (g).

3. Results and discussion

3.1. Characteristics of the adsorbent material

The physico-chemical properties of LVM are shown in Table 1. SiO_2 and Al_2O_3 are the major constituents of the LVM, although other oxides are present in smaller amounts. The surface morphology of the LVM was observed by FESEM analysis (Fig. 1). The image shows that LVM particles are soft clumps that are mainly composed of irregular and porous particles. X-ray diffraction (XRD) can be used to determine the bulk structure of a material and can also provide information about the composition of a material that has a crystalline structure. The XRD pattern of LVM shows that the majority of this material is an amorphous phase (Fig. 2). Also, quartz accounts for the crystal phase that is present in the LVM.

3.2. Adsorption studies

3.2.1. The effect of pretreating the adsorbent

Pretreatment of the adsorbent (e.g., autoclaving, drying, and washing with acid or base) enhances the adsorption efficiency [15]. Herein, the adsorption capacities of LVM samples that were exposed to washing and calcination pretreatments were compared (Fig. 3). The washed and calcined LVM had higher adsorption capacity than wet LVM, and the highest adsorption capacity (110.26 mg g^{-1}) was achieved with LVM that had been washed and calcined (after 30 min of contact time). This excellent adsorption capacity can be attributed to the fact that the organic impurities adsorbed on the surface of wet LVM were eliminated during the calcination at 550 °C; as a result, the surface area increased, which enabled better adsorption of MO. In addition, throughout the heating process, calcium oxide in the LVM might be converted to a porous Ca-based material, which may enhance the adsorption capability of the LVM [16]. Therefore, this washing and calcining procedure was applied to the LVM that was used in the subsequent studies.

3.2.2. The effect of pH

MO exists in a basic form when dissolved in aqueous solutions (Fig. 4a). In a solution becoming more acidic, its color changes from yellow to orange and finally to red with pH from 4.4 to 3.1. The adsorption band at 464 nm in acidic solution of MO should be assigned to the contribution of hydrazone structure to the resonance (Fig. 4b) [17].

The pH of the solution is one of the most important process parameters for controlling the adsorption. Fig. 5 shows the effect of pH value (in the range of pH = 3–10) on the adsorption of MO onto

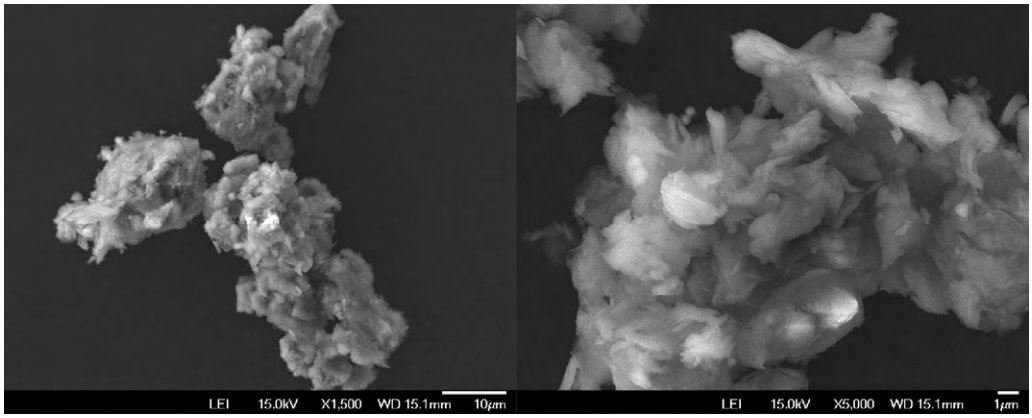

Fig. 1. Scanning electron microscopic images of LVM.

LVM. The maximum adsorption capacity (66 mg g^{-1}) was attained at pH 3. According to Table 1, the major constituents of LVM are SiO_2 and Al_2O_3, which develop charges when in contact with water [3]. Protonation of the silica present in LVM likely occurred, facilitating diffusion and providing a more active LVM surface. Al_2O_3, a typical amphoteric oxide, dissolves in a strong acid to give Al^{3+} ions which then attracted to more stable negatively charged MO molecules (Fig. 4b), resulting in greater adsorption. However, the adsorption capacities decreased significantly when the pH of the system was increased, and remained nearly constant over the pH values of 5–10. The higher pH value reduced the number of positively charged sites and raised the number of negatively charged sites, creating electrostatic repulsion between the negatively charged surface of the LVM and the anionic MO molecules. As a result, there was in a significant reduction in the removal of MO from the solu-

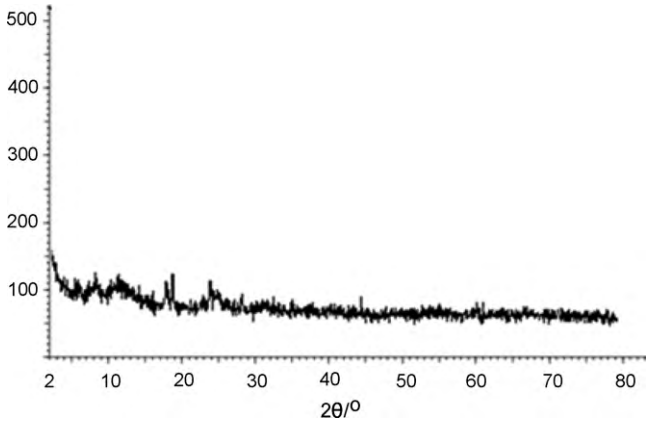

Fig. 2. XRD pattern of Lapindo volcanic mud.

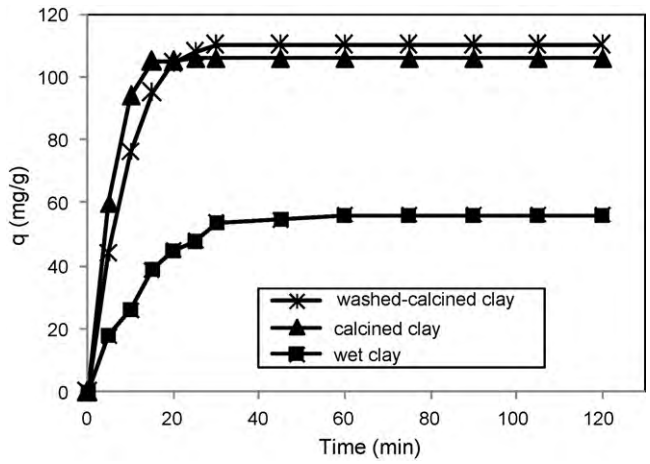

Fig. 3. Effect of LVM pretreatment (initial concentration 200 mg L^{-1}, adsorbent dosage 0.5 g L^{-1}, initial pH 3).

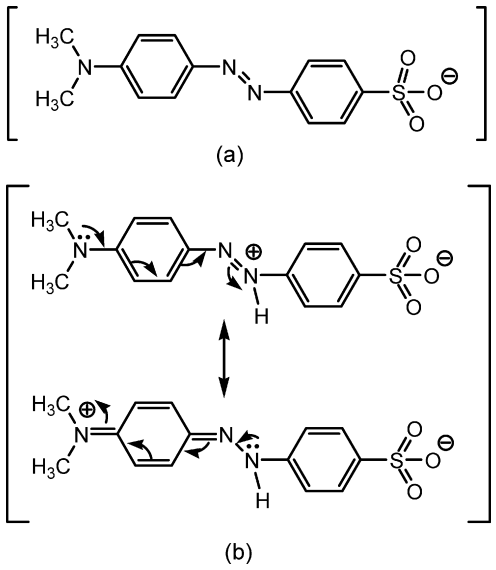

Fig. 4. (a) Basic and (b) acidic structures of methyl orange.

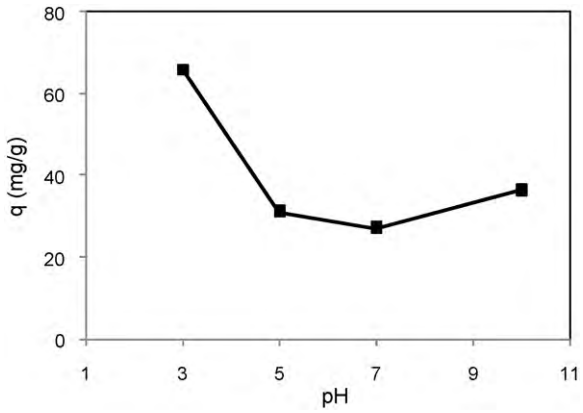

Fig. 5. Effect of pH on adsorption of MO on LVM (adsorbent dosage 2.0 g L^{-1}, initial MO concentration 100 mg L^{-1}).

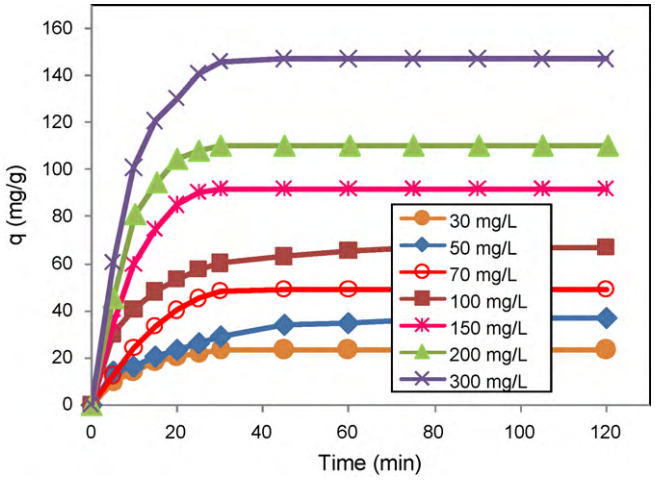

Fig. 6. Effect of initial concentration of the MO on LVM (adsorbent dosage 0.5 g L^{-1}, initial pH 3).

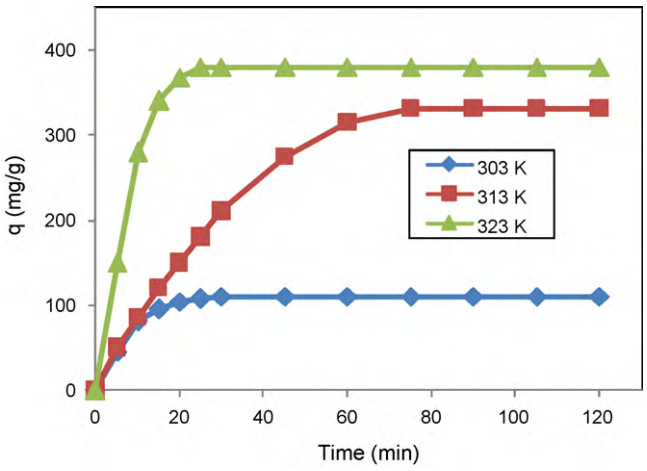

Fig. 8. Effect of temperature on adsorption of MO onto LVM (initial concentration 200 mg L^{-1}, initial pH 3, adsorbent dosage 0.5 g L^{-1}, contact time 2 h).

tion. Moreover, the presence of some alkali metal oxides in LVM also provided an abundance of hydroxyl anions when the material was in contact with water, and these anions competed with the anionic MO molecules for the adsorption sites, which resulted in lower adsorption of MO [18].

3.2.3. The effect of initial MO concentration

Experiments were carried out at different initial concentrations of MO while the other parameters were kept constant. As shown in Fig. 6, the adsorption capacity improved with increased initial dye concentrations. A higher initial dye concentration led to an increase in the mass gradient between the solution and the LVM, which then functions as a driving force for the transfer of dye molecules from bulk solution to the LVM surface [3]. At an MO concentration of 300 ppm, the maximum adsorption capacity was 150 mg g^{-1} after a contact time of 30 min.

3.2.4. The effect of adsorbent dosage

Fig. 7 shows the effect of varying the adsorbent dosage from 0.25 to 2 g L^{-1} of LVM. The adsorption capacity of MO increased with decreasing adsorbent dosage, and the highest adsorptive capacity (110 mg g^{-1}) was achieved using 0.25 g L^{-1} of LVM. A lower absorbent dosage means that a smaller overall total surface area of LVM is exposed, and hence, more MO anions were adsorbed onto the surface per gram unit of LVM, which led to the higher adsorption capacity.

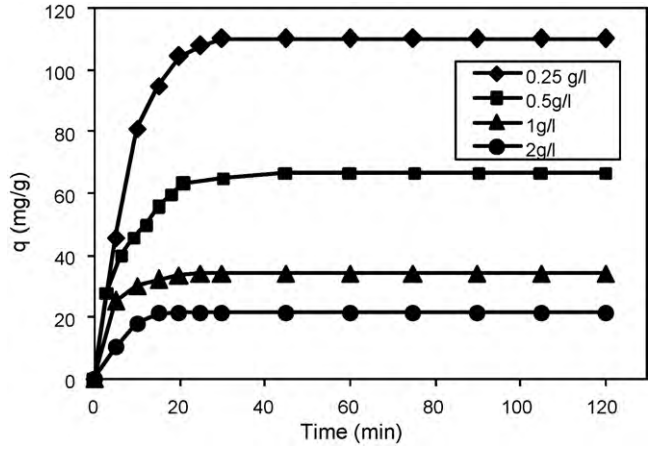

Fig. 7. Effect of LVM dosage (initial concentration 100 mg L^{-1}, initial pH 3).

3.2.5. The effect of temperature

The effect of temperature on MO adsorption of four different initial concentrations (50, 100, 200 and 300 mg L^{-1}) was studied in the temperature range of 303–323 K, and the results were shown for 200 mg L^{-1} initial concentration as an example in Fig. 8. It was observed that the adsorption capacity of MO increased with increase in temperature may be due to the enlargement of the pore sizes of adsorbent particles at elevated temperatures. Similar trends also observed for all concentration of MO solutions studied, indicating endothermic nature of the adsorption of MO onto LVM [19].

3.3. Adsorption isotherms

In this study, two commonly used models, the Freundlich [20] and Langmuir [21] isotherms were applied to understand the dye–clay interaction. The Freundlich isotherm is an empirical equation that assumes that the adsorption surface becomes heterogeneous during the course of the adsorption process. The heterogeneity arises from the presence of different functional groups on the surface and from the various adsorbent–adsorbate interactions. The Freundlich isotherm is expressed by the following empirical equation:

$$q_e = K_F C_e^{1/n} \quad (2)$$

In logarithmic form, Eq. (2) can be represented as

$$\log q_e = \log K_F + \frac{1}{n} \log C_e \quad (3)$$

where q_e is the amount of MO adsorbed per unit of adsorbent at equilibrium (mg g^{-1}), C_e is the concentration of the dye solution at equilibrium (mg L^{-1}), K_F and n are Freundlich adsorption isotherm constants, which indicate the extent of the adsorption and the degree of nonlinearity between the solution concentration and the adsorption, respectively. The values of K_F and n can be calculated from the intercept and slope of the linear plot between log C_e and log q_e (Fig. 9a) and are listed in Table 2. In general, as the K_F value increases, the adsorption capacity of the adsorbent for a given adsorbate also increases. The value of the Freundlich exponent n (2.247) is in the range of $n > 1$, indicating that the adsorption process is favorable [22].

The Langmuir adsorption model is based on the assumption that the maximum adsorption corresponds to a saturated monolayer of

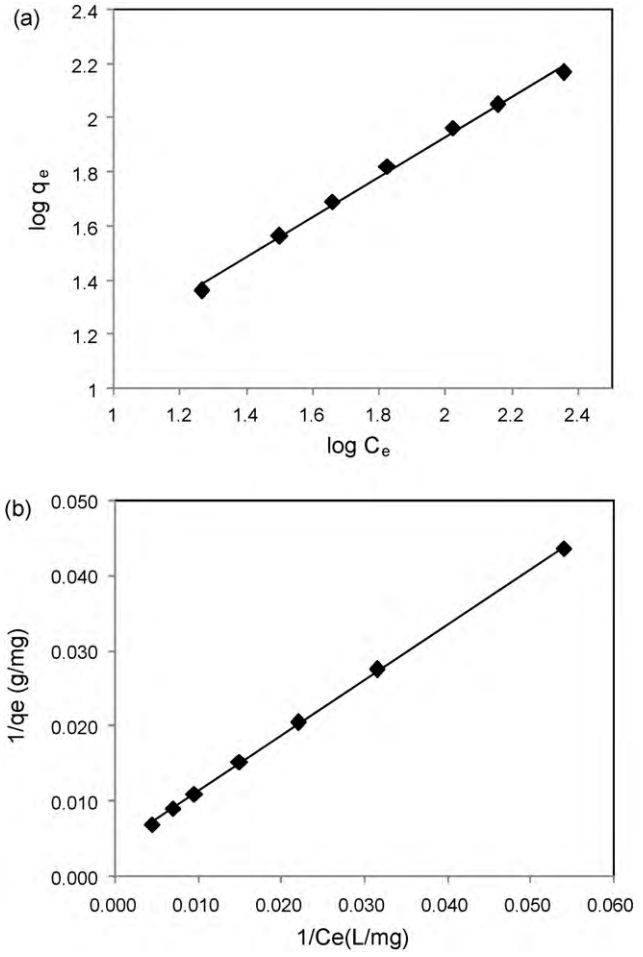

Fig. 9. Adsorption isotherm for adsorption of MO on LVM (adsorbent dosage 0.5 g L^{-1}, initial pH 3): (a) Freundlich and (b) Langmuir.

solute molecules on the adsorbent surface. The equation is given as

$$q_e = \frac{q_m K_L C_e}{1 + K_L C_e} \quad (4)$$

The linear form of Eq. (4) can be described by

$$\frac{1}{q_e} = \frac{1}{q_m} + \frac{1}{q_m K_L}\frac{1}{C_e} \quad (5)$$

where C_e is the concentration of dye solution at equilibrium (mg L^{-1}), q_e is the amount of MO adsorbed per unit of adsorbent at equilibrium (mg g^{-1}), q_m is the maximum amount of adsorption with complete monolayer coverage on the adsorbent surface (mg g^{-1}), and K_L is the Langmuir constant, which is related to the energy of adsorption (L mg^{-1}). The Langmuir constants K_L and q_m can be determined from the intercept and slope of the linear plot of $1/q_e$ versus $1/C_e$ (Fig. 9b) and are presented in Table 2.

Table 2
Isotherm parameters for adsorption of methyl orange on Lapindo volcanic mud at 30 °C.

Isotherm	Parameters
Freundlich	
K_F	5.5208
n	2.247
R^2	0.995
Langmuir	
q_m (mg g^{-1})	333.33
K_L (L mg^{-1})	0.00407
R^2	0.999
R_L	0.450

Table 3
Comparison of maximum adsorption capacities of various adsorbents for methyl orange.

Adsorbent	Contact time (min)	q_m (mg g^{-1})	Reference
Activated alumina	–	9.8	[23]
De-oiled soya	150 min	16.7	[24]
Bottom ash	4 h	3.6	[24]
Zn/Al-LDO	2 h	181.9	[25]
Banana peel	24 h	21	[26]
Orange peel	24 h	20.5	[26]
Lapindo volcanic mud	25 min	333.33	This study

The essential characteristics of the Langmuir isotherm can be expressed in terms of a dimensionless constant separation factor R_L [22], which is given by Eq. (6)

$$R_L = \frac{1}{1 + K_L C_0} \quad (6)$$

where C_0 (mg L^{-1}) is the highest initial concentration of adsorbent, and K_L (L mg^{-1}) is the Langmuir constant. The parameter R_L indicates the nature of shape of the isotherm accordingly:

$R_L > 1$	Unfavorable adsorption
$0 < R_L < 1$	Favorable adsorption
$R_L = 0$	Irreversible adsorption
$R_L = 1$	Linear adsorption

Table 2 shows that the value of R_L is 0.450 at 30 °C, indicating that the adsorption of MO on LVM is favorable at the temperature studied. The R^2 values of the Langmuir and Freundlich isotherms are 0.999 and 0.995, respectively, indicating that the equilibrium sorption data fits best with the Langmuir isotherm. This data confirms that the adsorption of MO on LVM occurs as a monolayer coverage process. A similar result was reported for adsorption of congo red dye on kaolin [18]. Table 3 lists a comparison of the maximum adsorption capacities (q_{max}) of MO on various adsorbents. LVM has a relatively large adsorption capacity (333.33 mg g^{-1}), suggesting that it may be a promising material for the removal of azo dyes from aqueous solutions.

3.4. Adsorption kinetics

Adsorption kinetic models were used to acquire a better understanding of the mechanism by which the dye is adsorbed from aqueous solutions by LVM. In this study, three models were used to investigate the details of the MO adsorption process onto LVM: the Lagergren pseudo-first-order model [27], the Ho pseudo-second-order model [28] and the intraparticle diffusion model.

3.4.1. The pseudo-first-order model

The Lagergren pseudo-first-order model is based on the assumption that the rate of change of solute uptake over time is directly proportional to the difference in saturation concentration and the amount of solid uptake over time:

$$\frac{dq_t}{dt} = k_1(q_e - q_t) \quad (7)$$

Intergrating Eq. (7) and noting that $q_t = 0$ at $t = 0$ gave following equation:

$$\log(q_e - q_t) = \log q_e - \frac{k_1 t}{2.303} \quad (8)$$

where q_t is the amount of dye adsorbed per unit of adsorbent (mg g^{-1}) at time t, k_1 is the pseudo-first-order rate constant (min^{-1}), and t is the contact time (min). The adsorption rate con-

Table 4
Adsorption kinetic parameters for the adsorption of methyl orange on Lapindo volcanic mud at different initial concentrations.

C_0 (mg L^{-1})	$q_{e,exp}$ (mg/g)	Pseudo-first order			Pseudo-second order			
		q_e (mg g^{-1})	k_1 (1/min)	R^2	q_e (mg g^{-1})	k_2 (g/mg min)	R^2	h (mg/g min)
300	146.83	199.54	0.150	0.936	166.67	0.00144	0.998	40.002
200	110.26	130.06	0.154	0.991	125.00	0.00246	0.998	38.438
150	91.68	124.45	0.157	0.951	100.00	0.00244	0.997	24.400
100	66.00	56.10	0.067	0.990	71.43	0.00211	0.999	10.766
70	49.00	71.78	0.122	0.928	55.56	0.00203	0.990	6.266
50	36.00	35.65	0.055	0.980	41.67	0.00184	0.995	3.195
30	22.95	25.76	0.120	0.968	24.39	0.00940	0.997	5.592

stant (k_1) was calculated from the plot of $\log(q_e - q_t)$ versus t (Table 4).

3.4.2. The pseudo-second-order model

The Ho pseudo-second-order model is presented as

$$\frac{dq_t}{dt} = k_2(q_e - q_t)^2 \quad (9)$$

and when $q_t = 0$ at $t = 0$, Eq. (9) can be integrated into following equation:

$$\frac{t}{q_t} = \frac{1}{k_2 q_e^2} + \frac{t}{q_e} \quad (10)$$

where k_2 is the pseudo-second-order rate constant (g mg^{-1} min^{-1}). The initial adsorption rate, h (mg g^{-1} min^{-1}), at $t = 0$ is defined as

$$h = k_2 q_e^2 \quad (11)$$

The values of h, q_e and k_2 can be obtained from the linear plot of t/q_t versus t (Fig. 10).

According to Eq. (8), the plot of $\ln(q_e - q_t)$ versus t, and Eq. (10), the plot of t/q_t versus t should each give a straight line. Table 4 shows both rate constants (k_1 and k_2) and the corresponding linear regression correlation coefficient values (R^2) for both models. The highest values of R^2 were observed with the pseudo-second-order model ($R^2 > 0.995$ for all concentrations), and the theoretical q_e values obtained from this model were also closer to the experimental $q_{e,exp}$ values at different initial MO concentrations. These results indicate that the pseudo-second-order kinetic model gave a better correlation for the adsorption of MO on LVM compared to the pseudo-first-order model. Similar results have been observed in the adsorption of congo red onto bentonite, kaolin and zeolite [18].

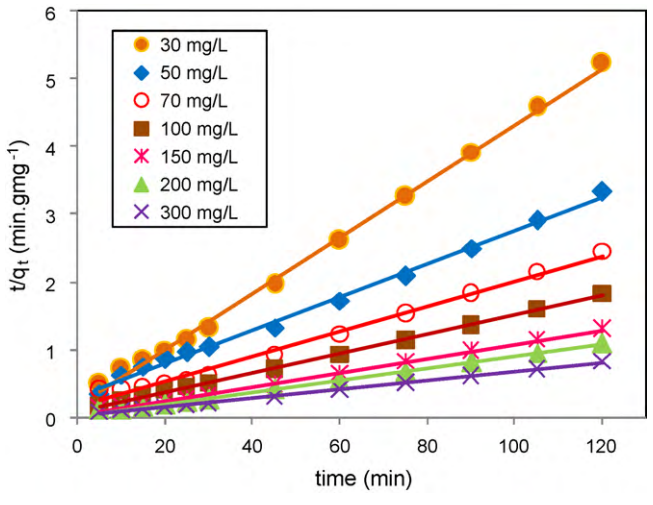

Fig. 10. Pseudo-second-order kinetic for adsorption of MO on LVM (adsorbent dosage 0.5 g L^{-1}, initial pH 3).

3.4.3. The intraparticle diffusion model

To identify the mechanism by which MO diffuses to the LVM surface (this information will be particularly useful for design purposes), the kinetic results were analyzed using the Weber and Morris intraparticle diffusion model [29],

$$q_t = k_{id} t^{1/2} + C \quad (12)$$

where k_{id} is the intraparticle diffusion rate constant (mg g^{-1} min$^{-1/2}$) and C is the slope that represents the thickness of the boundary layer. According to this model, a plot of the amount of dye adsorbed (q_t) versus the square root of time ($t^{1/2}$) should be linear, and if these lines pass through the origin, then the intraparticle diffusion is the only rate-controlling step [30]. However, as shown in Fig. 11, the plots are not linear over the whole time range and, instead, can be separated into multi-linear curves, illustrating that multiple stages were involved in the adsorption process. The first sharper line represents the surface adsorption, the second line corresponds to the intraparticle diffusion and the third line indicates the final equilibrium stage of adsorption, where the intraparticle diffusion starts to slow down because most of the adsorption sites are saturated [31]. These multi-linear curves might be due to adsorption on the irregular, non-uniform sites in the steps and edges of the LVM particles, as shown by the SEM photographs in Fig. 1.

3.5. Thermodynamic analyses of the adsorption isotherm data

Thermodynamic parameters such as the changes in the standard free energy (ΔG°), enthalpy (ΔH°) and entropy (ΔS°) can be calculated using the following equations:

$$\Delta G^\circ = -RT \ln K_C \quad (13)$$

$$\Delta G^\circ = \Delta H^\circ - \Delta S^\circ T \quad (14)$$

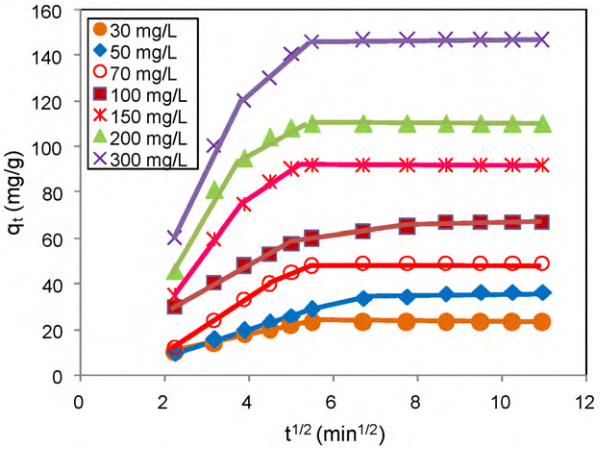

Fig. 11. Weber–Morris intraparticle diffusion plots for the adsorption of MO by LVM.

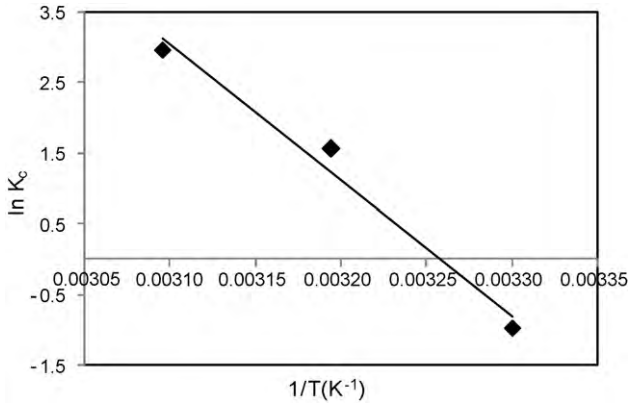

Fig. 12. Plot of $\ln K_C$ versus $1/T$ for estimation of thermodynamic parameters for the adsorption of MO onto LVM (initial concentration 200 mg L^{-1}).

Table 5
Thermodynamic parameters for the adsorption of methyl orange on Lapindo volcanic mud at different temperatures.

T (K)	$\ln K_C$	ΔG° (kJ mol^{-1})	ΔH° (kJ mol^{-1})	ΔS° (kJ mol^{-1} K^{-1})
303	−0.9661	2.434		
313	1.5579	−4.054	159.887	0.521
323	2.9532	−7.931		

where K_C is the equilibrium constant of the adsorption, which obtained from Eq. (15)

$$K_C = \frac{C_e(\text{adsorbent})}{C_e(\text{solution})} \quad (15)$$

where C_e(adsorbent) and C_e(solution) are the equilibrium concentration of the dye ions on adsorbent and in solution, respectively. Eqs. (13) and (14) then give the van't Hoff equation as

$$\ln K_C = \frac{\Delta S^\circ}{R} - \frac{\Delta H^\circ}{RT} \quad (16)$$

As shown in Fig. 12, the plot of $\ln K_C$ versus $1/T$ gives a straight line with a slope of ΔH° (kJ mol^{-1}) and an intercept of ΔS° (J mol^{-1} K^{-1}). The values of these thermodynamic parameters (studied at three different temperatures) are listed in Table 5.

The decrease in ΔG° values with increasing temperature indicates an increase in the feasibility and spontaneity of the adsorption at higher temperatures. The positive value of ΔG° at 303 K showed that the adsorption was not a spontaneous one and that the system gained energy from an external source [32,33]. The positive ΔH° value indicates the endothermic nature of the adsorption, and its magnitude which falls into a range of 80–200 kJ mol^{-1}, gives information about the type of chemisorption process [34]. This feature may also indicate that monolayer adsorption is taking place [35]. The positive values of ΔS° suggest that there is increased randomness at the solid–solution interface during the adsorption of MO in aqueous solution on LVM. Also, the positive value of ΔS° indicates that some structural changes may have taken place as a result of interactions between the MO molecules and the functional groups on the LVM surface [31].

4. Conclusion

The present study investigated the adsorption of MO from aqueous solutions by using an adsorbent of Lapindo volcano mud. LVM has been demonstrated to be highly effective for the removal of the anionic dye MO with an adsorption equilibrium time of less than 30 min. The best-fit adsorption isotherm was achieved with the Langmuir model, indicating that adsorption occurs by monolayer coverage. The positive enthalpy change for the adsorption process confirms the endothermic nature of the adsorption. Kinetic calculations show that the adsorption followed the pseudo-second-order model with a multi-step diffusion process. The low price and abundance of LVM make this material particularly promising for the removal of anionic dyes in industrial wastewater treatment.

Acknowledgements

Our gratitude goes to Ministry of Science, Technology and Innovation Malaysia for their financial supports under the Fundamental Research Grant (No. 78326). We are also grateful to the Hitachi Scholarship Foundation for their supports.

References

[1] N. Dizge, C. Aydiner, E. Demirbas, M. Kobya, S. Kara, Adsorption of reactive dyes from aqueous solutions by fly ash: kinetic and equilibrium studies, J. Hazard. Mater. 150 (2008) 737–746.
[2] L.G. Devi, S.G. Kumar, K.M. Reddy, C. Munikrishnappa, Photo degradation of Methyl Orange an azo dye by Advanced Fenton Process using zero valent metallic iron: influence of various reaction parameters and its degradation mechanism, J. Hazard. Mater. 164 (2009) 459–467.
[3] I.D. Mall, V.C. Srivastava, N.K. Agarwal, I.M. Mishra, Removal of congo red from aqueous solution by bagasse fly ash and activated carbon: kinetic study and equilibrium isotherm analyses, Chemosphere 61 (2005) 492–501.
[4] T. Robinson, B. Chandran, P. Nigam, Removal of dyes from a synthetic textile dye effluent by biosorption on apple pomace and wheat straw, Water Res. 36 (2002) 2824–2830.
[5] C. Namasivayam, D. Prabha, M. Kumutha, Removal of direct red and acid brilliant blue by adsorption on to banana pith, Bioresour. Technol. 64 (1998) 77–79.
[6] Y.S. Ho, W.T. Chiu, C.C. Wang, Regression analysis for the sorption isotherms of basic dyes on sugarcane dust, Bioresour. Technol. 96 (2005) 1285–1291.
[7] S.W. Won, S.B. Choi, Y.S. Yun, Performance and mechanism in binding of Reactive Orange 16 to various types of sludge, Biochem. Eng. J. 28 (2006) 208–214.
[8] C.C. Wang, L.C. Juang, T.C. Hsu, C.K. Lee, J.F. Lee, F.C. Huang, Adsorption of basic dyes onto montmorillonite, J. Colloid Interface Sci. 273 (2004) 80–86.
[9] S. Wang, Z.H. Zhu, Characterisation and environmental application of an Australian natural zeolite for basic dye removal from aqueous solution, J. Hazard. Mater. B136 (2006) 946–952.
[10] E. Bulut, M. Özacar, I.A. Şengil, Equilibrium and kinetic data and process design for adsorption of Congo Red onto bentonite, J. Hazard. Mater. 154 (2008) 613–622.
[11] M.H. Karaoğlu, M. Doğan, M. Alkan, Removal of cationic dyes by kaolinite, Micropor. Mesopor. Mater. 122 (2009) 20–27.
[12] A.S. Özcan, B. Erdem, A. Özcan, Adsorption of Acid Blue 193 from aqueous solutions onto BTMA-bentonite, Colloids Surf. A: Physicochem. Eng. Aspects 266 (2005) 73–81.
[13] D. Cyranoski, Indonesian eruption: muddy waters, Nature 445 (2007) 812–815.
[14] http://en.wikipedia.org/wiki/Sidoarjo_mud_flow, retrieved on 2009-06-22.
[15] Z. Aksu, Application of biosorption for the removal of organic pollutants: a review, Process Biochem. 40 (2005) 997–1026.
[16] T. Hanzlíček, M. Steinerová-Vondráková, Investigation of dissolution of aluminosilicates in aqueous alkaline solution under laboratory conditions, Ceram. Silik. 46 (2002) 97–103.
[17] A. Zhang, Y. Fan, Influence of adsorption orientation of methyl orange on silver colloids by Raman and fluorescence spectroscopy: pH effect, Chem. Phys. 331 (2006) 55–60.
[18] V. Vimonses, S. Lei, B. Jin, C.W.K. Chow, C. Saint, Kinetic study and equilibrium Isotherm analysis of Congo Red adsorption by clay materials, Chem. Eng. J. 148 (2009) 354–364.
[19] N. Guptaa, S.S. Amritphale, N. Chandra, Removal of Zn (II) from aqueous solution by using hybrid precursor of silicon and carbon, Bioresour. Technol. 101 (2010) 3355–3362.
[20] H.M.F. Freundlich, Über die adsorption in lösungen, Z. Phys. Chem. 57 (1906) 385–470.
[21] I. Langmuir, The adsorption of gases on plane surfaces of glass, mica and platinum, J. Am. Chem. Soc. 40 (1918) 1361–1403.
[22] K.R. Hall, L.C. Eagleton, A. Acrivos, T. Vermeulen, Pore- and solid-diffusion kinetics in fixed-bed adsorption under constant-pattern conditions, Ind. Enq. Chem. Fundam. 5 (1966) 212–223.
[23] Y. Iida, T. Kozuka, T. Tuziuti, K. Yasui, Sonochemically enhanced adsorption and degradation of methyl orange with activated aluminas, Ultrasonics 42 (2004) 635–639.
[24] A. Mittal, A. Malviya, D. Kaur, J. Mittal, L. Kurup, Studies on the adsorption kinetics and isotherms for the removal and recovery of Methyl Orange from wastewaters using waste materials, J. Hazard. Mater. 148 (2007) 229–240.
[25] Z.M. Ni, S.J. Xia, L.G. Wang, F.F. Xing, G.X. Pan, Treatment of methyl orange by calcined layered double hydroxides in aqueous solution: adsorption property and kinetic studies, J. Colloid Interface Sci. 316 (2007) 284–291.

[26] A. Gurusamy, R.-S. Juang, D.-J. Lee, Use of cellulose-based wastes for adsorption of dyes from aqueous solutions, J. Hazard. Mater. B92 (2002) 263–274.
[27] S. Lagergren, About the theory of so-called adsorption of soluble substances, Kungliga Svenska Vetenskapsakademiens, Handlingar 24 (1898) 1–39.
[28] Y.S. Ho, G. McKay, Pseudo-second order model for sorption processes, Process Biochem. 34 (1999) 451–465.
[29] W.J. Weber Jr., J.C. Morris, Kinetics of adsorption on carbon from solution, J. Sanit. Eng. Div. Am. Soc. Civ. Eng. 89 (1963) 31–60.
[30] K.G. Bhattacharyya, A. Sharma, Kinetics and thermodynamics of Methylene Blue adsorption on Neem (*Azadirachta indica*) leaf powder, Dyes Pigments 65 (2005) 51–59.
[31] K.G. Bhattacharyya, A. Sharma, Adsorption of Pb(II) from aqueous solution by *Azadirachta indica* (Neem) leaf powder, J. Hazard. Mater. B113 (2004) 97–109.
[32] N. Atar, A. Olgun, Removal of acid blue 062 on aqueous solution using calcinated colemanite ore waste, J. Hazard. Mater. 146 (2007) 171–179.
[33] A. Özcan, E.M. Öncü, A.S. Özcan, Kinetics, isotherm and thermodynamic studies of adsorption of Acid Blue 193 from aqueous solutions onto natural sepiolite, Colloids Surf. A: Physicochem. Eng. Aspects 277 (2006) 90–97.
[34] Y. Liu, Y.-J. Liu, Biosorption isotherms, kinetics and thermodynamics—review, Sep. Purif. Technol. 61 (2008) 229–242.
[35] Y. Seki, K. Yurdakoç, Adsorption of promethazine hydrochloride with KSF montmorillonite, Adsorption 12 (2006) 89–100.